Polymer Journal , Vol. 2, No. 6, pp 768—782 (1971)

Pressure—Strain and Pressure—Volume Relationships in the Crystal Lattice of Polyethylene at 293°K

Taisuke ITO and Harumasa MARUI*

Department of Dyeing, Faculty of Industrial Arts, Kyoto University of Industrial Arts and Textile Fibers, Matsugasaki, Sakyo-ku, Kyoto, Japan.

(Received April 19, 1971)

ABSTRACT: A high-pressure X-ray diffraction cell was developed, capable of causing X-ray diffraction of a specimen placed under purely hydrostatic high pressures up to 5000kg/cm². From the shifts of the diffraction lines induced by these pressures, the strain (ε) of an interplanar spacing (d_0) ($\varepsilon=\Delta d/d_0$) was obtained and plotted against pressure.

A high-density polyethylene (PE) was used for the measurements at 293°K. The crystal lattice of PE deforms in an elastic manner within a strain of 3% and by a time scale of the X-ray exposures. The orthorhombic crystal structure of PE remains constant under pressure, in spite of the extremely anisotropic crystal deformations.

For pressures less than 3000kg/cm², the pressure *vs.* ε relationship was found to be expressed in the three principal axis directions by the following equations:

a-axis direction: $-\varepsilon_{200}=11.5\times10^{-6}p-0.120\times10^{-8}p^2$

b-axis direction: $-\varepsilon_{020}=7.3\times10^{-6}p-0.019\times10^{-8}p^2$

c-axis (fiber axis) direction: $-\varepsilon_{c\text{-axis}}=0.30\times10^{-6}p-0.0032\times10^{-8}p^2$

The pressure *vs.* volumetric compression relationship can be obtained by summing ε's in the principal axis directions as follows.

$$-\Delta V/V_0=19.1\times10^{-6}p-0.143\times10^{-8}p^2$$

The results so formulated are discussed in terms of mechanical anisotropy of linear compressibility, volumetric compressibility, the C_2 parameter defined by Barker and the Grüneisen parameter.

KEY WORDS Pressure / Crystal Lattice / X-ray Diffraction / Strain / Volume / Compressibility / Polyethylene / Anisotropy / Anharmonicity / Grüneisen Parameter /

In recent years a considerable body of theory has been developed which makes it possible to understand the compressibility and the Grüneisen parameter of the crystal of polymers. Müller[1] calculated the compressibility of the paraffin crystal based on the results of his systematic investigations on the crystal structure of paraffins, and predicted a reasonable value for the compressibility, which agreed closely with the values found experimentally by X-ray diffraction. In 1957 Brandt[2] calculated the 0°K compressibility of crystals of five linear polymers using a Lennard-Jones 12-6 potential and the dipole interaction terms and obtained, for polyethylene(PE), an excellent agreement between theory and Bridgman's compression data for pressures up to 40000kg/cm² (extrapolated to 0°K). Barker[3] made a systematic study of the relationships between the Grüneisen parameter, the elastic modulus and intermolecular potential of the polymeric solids and metals. Barker's work was recently extended by Broadhurst and Mopsik[4] who predicted isothermal bulk modulus *vs.* volume relations for high-density PE and paraffins around room temperature, in reasonable

* Present address: *Research Center, Dai-ichi Kogyo Seiyaku Co., Ltd., Nishi-Shichijo, Shimokyo-ku, Kyoto, Japan.*

agreement with experimental data. Recently, Odajima, and Maeda[5] and Pastine[6] made approaches taking into account the detail of the crystal structure of PE. The former authors applied Born and Huang's dynamical theory of the crystal lattice on the PE crystal, and found the compressibility at 20°C became 1.99×10^{-11}cm^2/dyn and 2.72×10^{-11} cm^2/dyn according to two differents sets of calculations. Pastine gave p, V, T equations of state for purely crystalline and purely amorphous PE, and combined the two according to the degree of crystallinity.

In contrast to the theoretical approaches reviewed above, it seems rather few works have been published, since Müller's paper[1] in 1941, on the experimental investigations of the compressibility of the crystal lattice of polymers. Weir and Hoffman[7] measured by piezometry the compressibility of the bulk specimen of the normal hydrocarbons with carbon numbers ranging from 18 to 30, and concluded their average compressibility under atmospheric pressure to be 29.8×10^{-6}atm^{-1} at 21°C. Hellwege, Knappe, and Lehmann[8] studied, also by piezometry, the compressibility of high- and low-density PE and found, by extrapolation to 100-% crystallinity, the compressibility for 100-% crystalline PE to be 1.6×10^{-5}cm^2/kg.

In the above situations there is need for more detail and more direct experimental determinations of the compressibilities of the *crystal lattice* of polymers. The present paper describes, firstly, an experimental technique using X-ray diffraction to measure the pressure—strain behavior and to determine the pressure—volume relations of the crystal lattice of polymers and, secondly, details of the behavior of the crystal lattice of PE and *n*-heptacosane(*n*-$C_{27}H_{56}$) when subjected to hydrostatic pressures.

APPARATUS[10,14,15]

A high-pressure X-ray camera of piston-cylinder type was developed based on Kabalkina and Vereshchagin's camera[9] capable of supplying X-ray diffraction photographs of a specimen placed under purely hydrostatic high pressures reaching up to, at present, 5000kg/cm^2. The camera consists essentially of a high-pressure cell made from Maraging steel and a moving-film multiple exposure X-ray camera of a semi-cylindrical type. The high-pressure cell is shown in cross section in Figure 1. The X-ray beam, filtered and collimated by a pinhole unit(A), passes through the beryllium window(B) and meets the specimen placed in an axial circular hole drilled into the beryllium window. The hole is 1mm in diameter and 8mm deep and its central axis (vertical), coincidental with the axis of the camera, is perpendicular to the incident X-ray beam. The equatorial zone of the diffracted X-rays, which pass through the horizontal aperture (C) 2mm in width and having a 2θ angle of approximately 55° on one side and 85° on the other side of the incident beam, are again limited by a long horizontal slit 1.9mm in width, and fall on a semicylindrical film which can be moved vertically by means of a fine screw device. The camera, described elsewhere,[10] is capable of making fifteen exposures on the same film for the specimen under atmospheric as well as high pressures. The spacing between any exposed zones (each 1.9mm in width) can be set up with an accuracy of $\pm$0.01mm by knowing the height of the film, with two 1/100-mm dial gauges. It is thus possible to make an arbitrary exposure program to choose the positions and the orders of zones to be exposed on a given film (4.3×20cm or 4.3×24cm). The camera was shown[10] to have a radius of 100.05 ± 0.02mm through all the exposure positions.

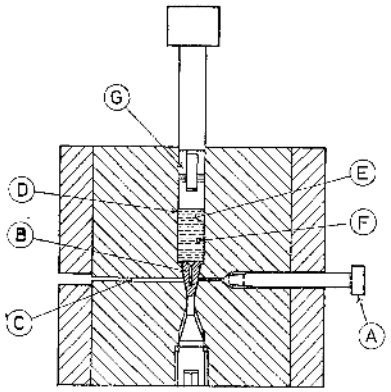

Figure 1. Schematic diagram of the hydrostatic high-pressure X-ray diffraction cell in cross section.

The high-pressure cell is mounted on the

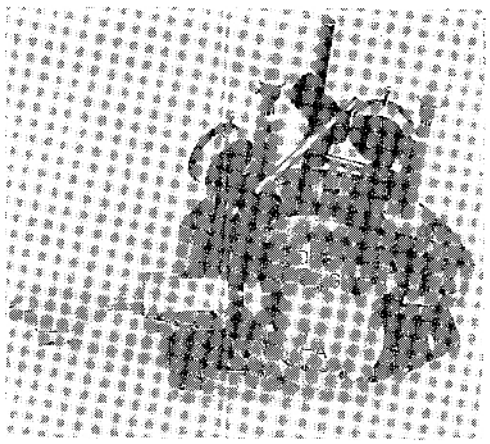

Figure 2. Photograph showing the high-pressure cell equipped with the high-pressure gauge and mounted on the multiple exposure camera: A, pinhole collimator; D, cylinder; G, Bridgman seal. The horizontal aperture appears on the other side of the cell and out of sight in the photograph.

camera as shown in Figure 2 with the use of the fits among the circumference of the cell (100.00mm in diameter), a shallow circular groove (1mm in depth and 100.04mm in diameter) cut concentrically on the base disc of the camera 28mm in thickness and a large washer ring 2mm in thickness which has no clearance for the circumference of the cell. The washer ring can be fixed on the base disc of the camera by four screw bolts with a slight adjustable clearance to obtain the coincidence between the axis of the camera and that of the specimen. The camera and the mounted high-pressure cell are placed on a 20ton hydraulic press which is fixed on the desk of a Rigaku Denki Model D-8C X-ray generator, giving direct contact between the pinhole unit (A) of the high-pressure cell and the window of the X-ray tube holder. Since the diameter of the cylinder (D) of the high-pressure cell is 10mm, a force of at least 7.85 tons will be necessary to obtain pressure of 10000kg/cm^2.

No part of the apparatus gave any mechanical trouble during the high-pressure experiments. This was conclusively demonstrated[11] by using a diamond powder as the specimen and obtaining the 111 diffraction lines under pressures up to 3000kg/cm^2. There was found to be no shift in the 111 diffraction lines within the reading error of the comparator, a reasonable result expected from the compressibility of the diamond, and no significant mechanical strain of the apparatus leading to experimental error.

EXPERIMENTALS

Pressure Measurements

The pressure generated in the pressure medium (E), water in the case of polyethylene, was measured by introducing a portion of the pressure medium through a pinhole (F) into a Kobe Steel Model 10-W-C high-pressure gauge.[12] The strain produced on the high-pressure gauge was read with a Kyowa Dengyo Model PM-5L static strain meter. The calibration for the pressure—strain relationship of the high-pressure gauge, including the combined use with the strain meter, was performed at the Laboratory of Very High Pressures, Kobe Steel, Ltd., Kobe, by the use of a lever-type controlled-clearance piston gauge[13] which had an estimated limit of uncertainty of less than $\pm 0.015\%$ up to 10000 kg/cm^2. The calibration has been carried out periodically once every six months. The resultant pressure—strain relationships show an excellent and reproducible linearity.[14,15] The error of the pressure measurements is estimated to be less than $\pm 2\%$ for low pressures (<1000 kg/cm^2) and $\pm 1\%$ for high pressures (>1000 kg/cm^2). These error estimations include the errors due to pressure leaks during X-ray exposures. The residual strain of the high-pressure gauge, temporarily appearing when the pressure is released to the level of the atmospheric pressure after experiments under high pressures, was found to be negligibly small.

Sample

A plate of linear PE 3-mm thick was made from Sholex 6009 polymer (Showa Denko Co.) by molding in a laboratory press at 165°C, followed by quenching in an ice-water bath. This plate was drawn at 90°C in an air thermostat eight times the original length and annealed under fixed length at 100°C for 10min (density, 0.961g/cm^3 at 30°C, 78-% crystallinity) or 120°C for 3hr (density, 0.967g/cm^3 at 30°C, 82-% crystallinity). An unoriented annealed specimen was obtained by molding the polymer

in the press at 165°C, followed by cooling in the press to 120°C, annealing for 3hr at the same temperature and cooling to room temperature by shutting off the press heaters (density, 0.967g/cm^3 at 30°C, 82-% crystallinity). Commercially available n-$C_{27}H_{56}$ was recrystallized three times from toluene solutions. This specimen of n-$C_{27}H_{56}$ melted at 59.6—61.2°C.

Specimen for X-ray Measurements

A rod about 1mm in diameter and 12mm in length was shaped, with a razor blade, from the prepared samples. In practice, the rod specimen was made carefully so that it fitted smoothly to the cylindrical specimen holder of the beryllium cell. For the drawn samples, the axis of the rod specimen was taken to be parallel to the drawing direction in the case of the measurements for the 200, 020, and 110 reflections, and to be perpendicular to it for the 002 reflection. In order to obtain the 011 reflection in the horizontal level, as required by the geometry of the high-pressure X-ray camera, the axis of the rod specimen was prepared so as to be inclined at 71 degrees to the drawing direction. The 011 reflection of this specimen was preliminarily checked by a flat camera. The n-$C_{27}H_{56}$ was ground in an agate mortar for three minutes and packed into the cell of the beryllium window.

In the case of the rod specimens, there exists sufficient room between the specimen and the wall of the hole of the beryllium window for the pressure medium (water) to penetrate and, hence, the hydrostatic pressure for the specimen was secured. n-$C_{27}H_{56}$ is a soft substance by itself and the hydrostatic pressure was also secured as well.

Experimental Procedures

The X-ray patterns under normal pressure were obtained for a specimen which has no history of pressure applications. Usually, two to seven exposures under the normal pressure were registered on one film to obtain a direct comparison with the results obtained under high-pressure conditions. By careful comparison of the results obtained by repeated pressure applications and releases on the same specimen under pressures up to 3000kg/cm^2, identical results within the experimental error were obtained, and the effects of the history of pressure applications on the pressure—strain behavior of the crystal lattice of PE were shown to be negligible.[14,15]

After the exposures under normal pressure were finished, the exposure under the high pressures was begun with the lowest pressure. The pressure was raised over a period of 3min and a further 15min were allowed for equilibration before commencing X-ray exposure. When one exposure under high pressure was finished, the pressure was raised to the next lower value. Leaks were infrequent, and the pressure could be maintained constant within a change of less than $\pm 2\%$. When the pressure was released from 3000kg/cm^2, a residual pressure of not more than 50kg/cm^2 was some-times unavoidable because of the friction between the Bridgman seal (G in Figure 1) and the wall of the cylinder.

Using nickel-filtered copper radiation (40kV and 18mA) and for each condition of pressure, an X-ray exposure ranging from 15min (110 reflection of the drawn specimen) to 4hr (020 reflection of the drawn specimen) was required for satisfactory patterns. X-ray patterns of such high quality were often obtained as to be quite comparable to those obtained under normal conditions.

The 200, 020, 002, 110, and 011 reflections of PE were observed. All the measurements were carried out at 20 ± 1.5°C. The specimen-to-film distance was determined by calibration with a special gauge.[10] The peak shift $\Delta 2\theta$ due to pressure was obtained from the increase of the distance between the diffraction lines. The shift of the diffraction lines could be determined with an accuracy of ± 0.025mm by using a comparator constructed[10] in our laboratory after Klug.[16] The strain ε for a lattice spacing under a pressure was calculated by

$$\varepsilon = \frac{\Delta d}{d_0} = -\cot\theta_0 \Delta\theta \,, \qquad (1)$$

where d and θ are the lattice spacing and the Bragg angle, respectively, and the zero-subscripts mean the values at normal pressure. The experimental error for measuring ε as cited hereafter has a width of $\Delta\varepsilon = 2.5 \times \cot\theta_0 \times 10^{-4}$, corresponding to the maximum error width of 0.05mm in the determinations of the peak

shifts. For the planes (200), (020), (002), (110), and (011), it amounts to, respectively, 0.0012, 0.0008, 0.0003, 0.0013, and 0.0007.

RESULTS

A first example of the experimental results is given in Figure 3. Here the 100°C-annealed drawn specimen was used and the pressure was raised to 3000kg/cm^2 over a period of 60 sec, and kept constant for about 6hr. The initial exposure was started immediately after the pressure level was achieved; 8 more exposures were made under the pressure, and the last exposure was started immediatey after the pressure-release (under a residual pressure of 2kg/cm^2). In Figure 3 the strain ε of the 110 plane is plotted against the time at the middle of the exposure, while each exposure time was 15min. It is seen that the 110 spacing in the crystallites of the linear PE deforms in an elastic manner within the time of of 15min, by the action of the pressure of 3000kg/cm^2. The same conclusion was obtained for the 200 plane by examination of the 200 reflections recorded on the same film that gave the result in Figure 3.

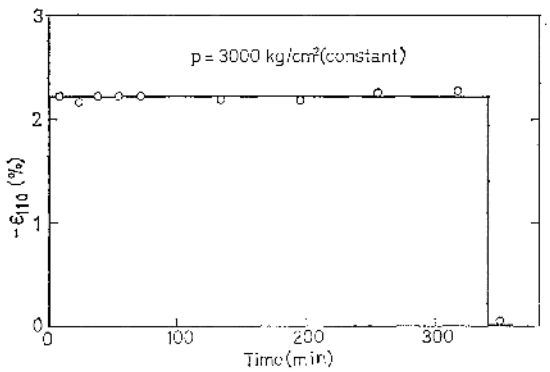

Figure 3. Strain of the 110 plane of drawn PE annealed at 100°C plotted against time under a constant pressure of 3000kg/cm^2, showing elastic response of the crystal lattice against pressure.

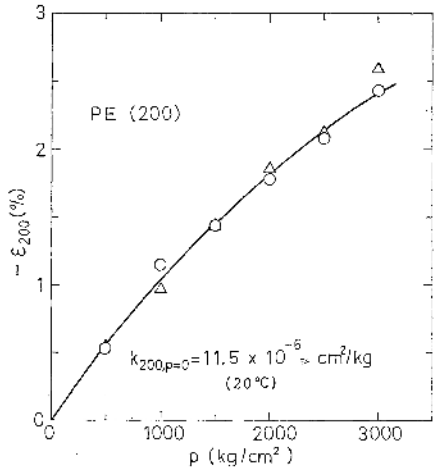

Figure 4. Pressure–strain curve for the 200 plane of drawn PE: ○, 120°C-annealed specimen; △, 100°C-annealed specimen.

Table I. $-\Delta d/d_0$ *vs.* pressure relationship at 20°C for the 200 plane of drawn high-density polyethylene annealed at 120°C

Pressure, kg/cm^2	$-\Delta d/d_0$	
	Observed	Calculated[a]
500	0.00527	0.00547
1000	0.0115	0.0103
1500	0.0144	0.0146
2000	0.0178	0.0183
2500	0.0208	0.0213
3000	0.0243	0.0238
35	0.0002	0.0004

[a] Calculated from eq 2.

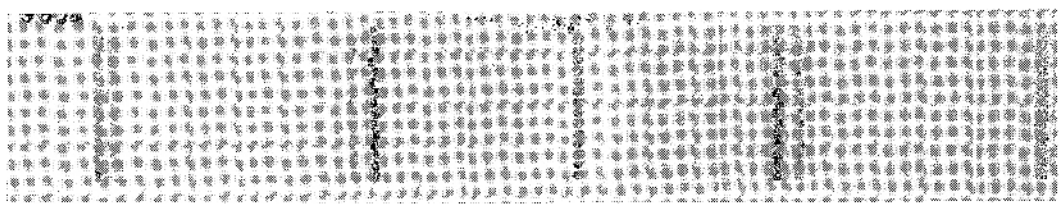

Figure 5. Pressure spectrum for the 110 and 200 reflections of 120°C-annealed drawn PE. Pressure (kg/cm^2): (from bottom) 1 (normal pressure), 500, 1, 1000, 1, 1500, 1, 2000, 1, 2500, 1, 3000, 1, and 35 (released from pressure of 3000kg/cm^2). Exposure time is 20 min for each exposed zone.

Figure 4 shows the pressure—strain curve for the 200 plane and Table I gives the numerical data. The results as calculated will be referred to in the next section. Figure 5 is the X-ray photograph which supplies the data for the 120°C-annealed specimen shown in Figure 4 and Table I. In Figure 5, 14 exposures in total were carried out, and the pressures applied (expressed in kg/cm^2) are, from bottom to top, 1 (the normal pressure), 500, 1, 1000, 1, 1500, 1, 2000, 1, 2500, 1, 3000, 1, and 35 (residual pressure when released from a pressure of 3000kg/cm^2), respectively. The reflections at the lowest angle are the 110, and those in the outer sides the 200 reflections, and the reflections appearing in the wider angles near to the edge of the film are due to the beryllium window. The 15th exposure zone was used for collimation and the diffraction lines recorded there are not important.

Figures 6 to 9 and Tables II and III are the results for the 020 and the 110 planes. In Figure 7, from which the data for the 020 plane of the 120°C-annealed drawn specimen shown in Figure 6 and Table II originate, the exposure time for each diffraction diagram was 4hr, but the 110 and 200 reflections were blocked out during most of the exposure by placing a brass shield in front of the film. The 110-data for the 120°C-annealed drawn specimen given in Figure 8 and Table III were supplied from Figure 5, while those for the unoriented specimen were provided from Figure 9. The X-ray photographs for the 100°C-annealed drawn specimens were not shown, because they show no basic difference from those for the 120°C-annealed drawn specimens (except that the former have a little denser background).

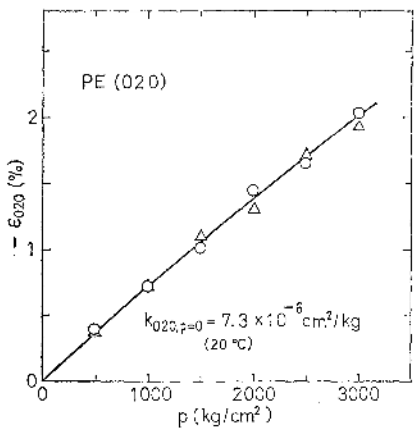

Figure 6. Pressure–strain curve for the 020 plane of drawn PE: ○, 120°C-annealed specimen; △, 100°C-annealed specimen.

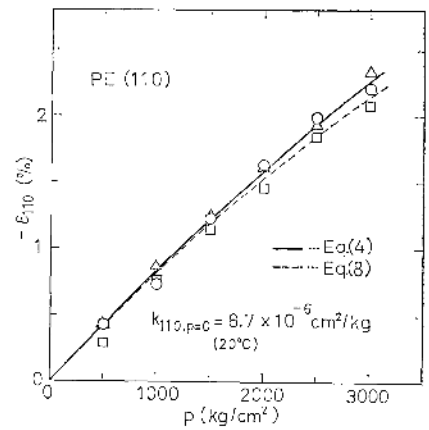

Figure 8. Pressure—strain curve for the 110 plane of PE: ○, 120°C-annealed drawn specimen; △, 100°C-annealed drawn specimen; □, 120°C-annealed unoriented specimen. Broken line was calculated from eq 8.

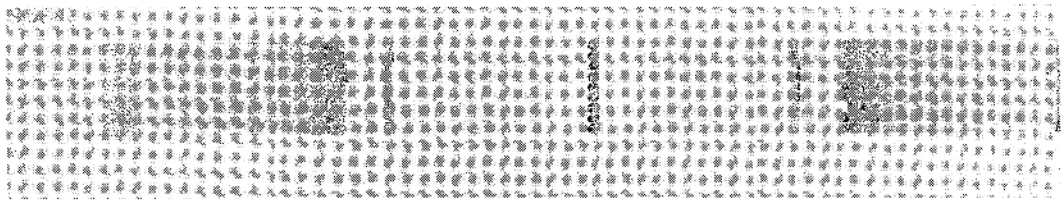

Figure 7. Pressure spectrum for the 110, 200, 210, 020, 120, and 310 reflections of 120°C-annealed drawn PE. Pressure (kg/cm^2): (from bottom) 1, 500, 1000, 1500, 2000, 2500, 3000, 1, and 1 (released pressure). Exposure time is 30min for the 110 and 200 reflections and 4hr for rest the reflections, for each exposed zone.

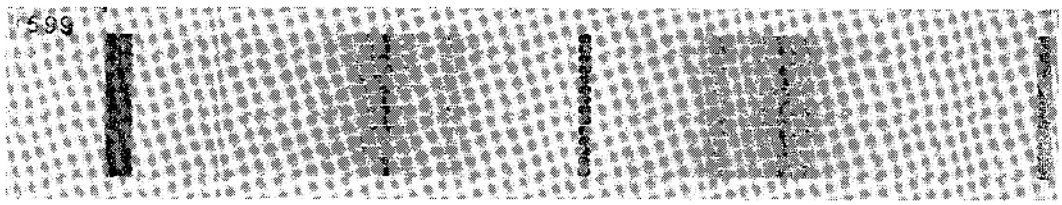

Figure 9. Pressure spectrum for the 110 and 200 reflections of 120°C-annealed unoriented PE. Pressure (kg/cm²): (from bottom) 1, 500, 1, 1000, 1, 1500, 1, 2000, 1, 2500, 1, 3000, 1 and 1 (released pressure). Exposure time is 60min for each exposed zone.

Table II. $-\Delta d/d_0$ *vs.* pressure relationship at 20°C for the 020 plane of drawn high density polyethylene annealed at 120°C

Pressure, kg/cm²	$-\Delta d/d_0$	
	Observed	Calculated[a]
500	0.00380	0.00360
1000	0.00706	0.00710
1500	0.0101	0.0105
2000	0.0145	0.0138
2500	0.0165	0.0170
3000	0.0203	0.0201
1	0.0000	0.0000

[a] Calculated from eq 3.

Table III. $-\Delta d/d_0$ *vs.* pressure relationship at 20°C for the 110 plane of drawn high density polyethylene annealed at 120°C

Pressure, kg/cm²	$-\Delta d/d_0$	
	Observed	Calculated[a]
500	0.00428	0.00424
1000	0.00731	0.00830
1500	0.0123	0.0122
2000	0.0163	0.0158
2500	0.0199	0.0193
3000	0.0221	0.0226
35	0.0008	0.0003

[a] Calculated from eq 4.

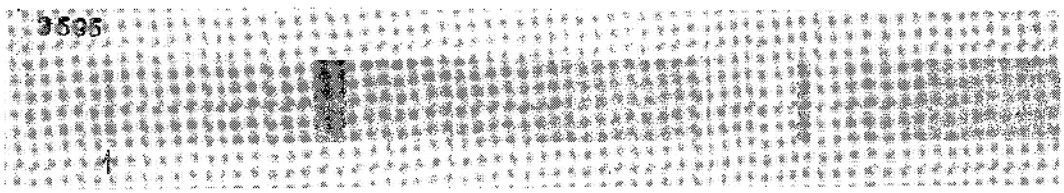

Figure 10. Pressure spectrum for the 002 reflection (indicated with arrow) of 100°C-annealed drawn PE. Pressure (kg/cm²): (from bottom) 1, 1000, 1, 2000, 1, 3000, 1 and 16 (released pressure). Exposure time is 60min for each exposed zone.

In Figure 10 the 002 reflection appears at a large angle of $2\theta=74.5°$. Many trial and error exposures were carried out to bring the specimen to the reflecting position for the 002 plane, by carefully rotating with a very small step and fixing the axis of the specimen. It was found that the 002 reflection moves only +0.12mm on the film with a pressure of 3000kg/cm² and this means a corresponding compressive strain of only 0.0008 per 3000kg/cm². The observed spacings for the 200 and 020 planes at normal pressure were 3.702 and 2.466Å, respectively (obtained from Figures 5 and 7), in complete

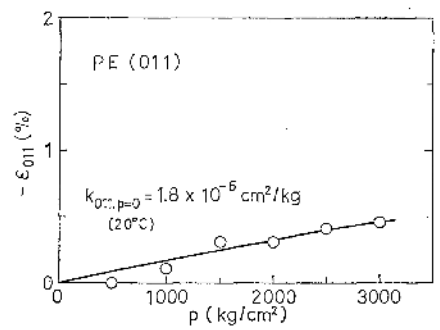

Figure 11. Pressure–strain curve for the 011 plane of 120°C-annealed drawn PE.

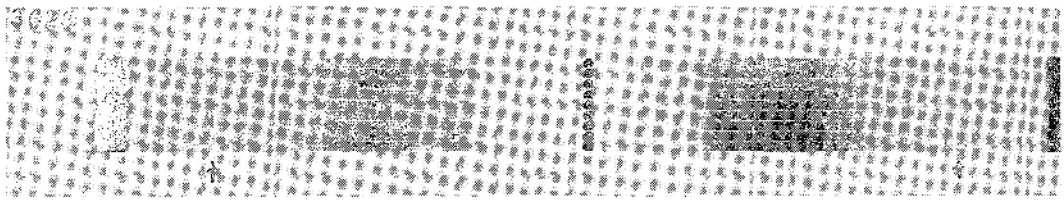

Figure 12. Pressure spectrum for the 011 reflection (indicated with arrow) of 120°C-annealed drawn PE. Pressure (kg/cm²): (from bottom) 1, 500, 1000, 1500, 2000, 2500, 3000, 1 and 16 (released pressure). Exposure time is 165min for each exposed zone.

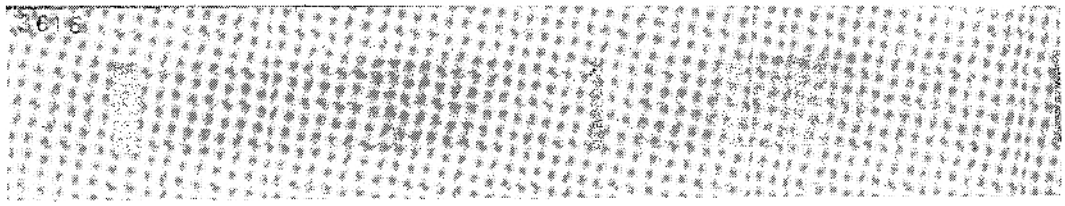

Figure 13. Pressure spectrum for the 110 and 200 reflections of n-$C_{27}H_{56}$. Pressure (kg/cm²): (from bottom) 1, 500, 1000, 1500, 2000, 2500, 3000, 1 and 43 (released pressure). Exposure time is 80min for each exposed zone.

Table IV. $-\Delta d/d_0$ *vs.* pressure relationship at 20°C for the 011 plane of drawn high density polyethylene annealed at 120°C

Pressure, kg/cm²	$-\Delta d/d_0$	
	Observed	Calculated[a]
500	0.0000	0.00086
1000	0.0011	0.0017
1500	0.0031	0.0025
2000	0.0031	0.0033
2500	0.0041	0.0040
3000	0.0046	0.0047
16	0.0005	0.00003

[a] Calculated from eq 5.

Table V. $-\Delta d/d_0$ *vs.* pressure relationship at 20°C for the 200 and the 110 planes of n-heptacosane (n-$C_{27}H_{56}$)

Pressure, kg/cm²	$-\Delta d/d_0$	
	(110)	(200)
500	0.00551	0.00682
1000	0.00904	0.0121
1500	0.0134	0.0154
2000	0.0165	0.0195
2500	0.0194	0.0212
3000	0.0240	0.0254

agreement with the values reported by Bunn.[17] The observed 002 spacing of 1.27Å also agrees well with the value provided by Bunn, although it was determined using the images of the direct beam to measure the reflection angle.

Figures 11 and 12 and Table IV show the results for the 011 plane. The 011 reflections were seen to be clearer on the original X-ray film than those reproduced in Figure 12, giving

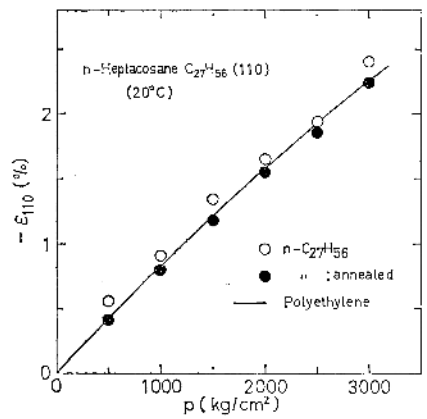

Figure 14. Pressure—strain plots for the 110 plane of n-$C_{27}H_{56}$ compared with the result of PE (solid line): ○, before annealing; ●, after annealing at 50°C for 5hr.

observed spacing under normal pressure of 2.231Å, in fairly close agreement with the value given by Bunn (2.25Å).

Figure 13 and Table V are for the n-$C_{27}H_{56}$ crystals and Figure 14 shows the pressure—strain curve for the 110 plane of n-$C_{27}H_{56}$ compared with that of PE. In Figure 14 were also shown the data for the specimen which was annealed, after the experiment for Figure 13, in the high-pressure cell at 50°C for 5hr without the pressure medium. This was done to check any pressure effect which might have been produced when the specimen was packed into the hole of the beryllium window. It may be seen from Figure 14 that such a possibility can be considered negligible within experimental error.

ANALYSIS OF THE RESULTS

In the following discussion it is assumed that a hydrostatic pressure which is equal to that generated in the pressure medium acts on each crystallite (or each crystal in the case of n-$C_{27}H_{56}$) distributed in the bulk of the specimen. This assumption is physically equivalent to stating that the amorphous regions transmit the pressure as a liquid medium. This role of transmitting pressure must be completed within a time of 15min since the X-ray exposure was begun on 15min equilibration after the pressure level was achieved.

According to elasticity theory, it is necessary that the hydrostatic pressure acting on any lattice plane is common and equal to the pressure acting on the crystallite. If either or both of the above assumptions and the requirement of the elasticity theory do not hold, nonhomogeneity of the pressure components is induced both around a crystallite and among each of the crystallites bathed in the incident beam. These should broaden the diffraction lines. Actually, such broadening of the diffraction lines due to the pressure applications is found to be negligible from considerable experimental evidence, not only in respect of PE but many other polymers not described here. An example will be seen from a reproduced photograph, as illustrated in Figure 5, where the diffraction lines *only* move, with good reproducible results,[14,15] by the pressure applications, giving a very simple character to the pressure-spectrum. Phase transition was not observed for pressures up to 3000kg/cm^2, which is the highest pressure level applied in the present experiment.

Osugi and Hara[18] showed that the density of a bulk specimen of Marlex 50 recovers almost completely to its original value when subjected to treatment under a very high pressure of 30000 atm at room temperature. Gruner, Wunderlich, and Bopp[19] also showed a complete recovery of the density of Marlex 50 bulk specimens after treatment under high pressure of 5.1kb (5200kg/cm^2) for 20hr, if the annealing temperatures were below 210°C. These results by Osugi, *et al.*, and by Gruner, *et al.*, are in close agreement with our results of the elastic recovery of the strain of the lattice spacing of PE against pressures, shown in Figure 3.

A preliminary check reveals that the pressure—strain plots obtained in the figures shown in the preceding section can be represented by a function $-\varepsilon=ap-bp^2$, where a and b are constants and p is pressure. Hence, by means of the least-squares method, the compressive strain data obtained by using the 120°C-annealed drawn specimen were fitted to the above equation and the following results* were obtained for each lattice plane observed.

a-axis direction:

$$-\varepsilon_{200}=11.5\times10^{-6}p-0.120\times10^{-8}p^2 \quad (2)$$

b-axis direction:

$$-\varepsilon_{020}=7.29\times10^{-6}p-0.0191\times10^{-8}p^2 \quad (3)$$

Normal direction to (110):

$$-\varepsilon_{110}=8.68\times10^{-6}p-0.0379\times10^{-8}p^2 \quad (4)$$

Normal direction to (011):

$$-\varepsilon_{011}=1.76\times10^{-6}p-0.00651\times10^{-8}p^2 \quad (5)$$

In the above relations the pressure is expressed in kg/cm^2 and the temperature corresponds to 20°C. In obtaining the relation for the 011 plane (eq 5), the first plot seen in Figure 11 at the pressure of 500kg/cm^2 was omitted from the least-squares. The result for the c-axis (fiber

* The results concerning the coefficients are slightly different from those published in ref 14 since the least-squares method was used in this paper.

axis) direction will appear later in eq 10. It should be emphasized that the above equations are designed to reproduce ε only within the range in which measurements were made ($p \leqq$ 3000kg/cm^2). Extrapolation in any sense may lead to serious errors, as shown by the zero or negative compressibility at or over the pressure making the first derivatives of the right-hand sides of the above equations zero.

The calculated strains according to eq 2—5 were shown in each of the tables and with a solid line, in each of the Figures for the pressure—strain relationship shown in the preceding section. It is seen in most instances that these equations, although originating from the data from the 120°C-annealed drawn specimen, can reproduce the experimental results to within the experimental error. Among them are included the data for the 100°C-annealed drawn specimen and the 120°C-annealed unoriented specimen. As seen in Figure 8, the ε_{110}-plots for the 120°C-annealed unoriented specimen appear to be slightly lower than those for the oriented specimens. Although the deviation seems to be within the experimental error, the assumption for the hydrostatically acting pressures mentioned in the first paragraph of this section might be affected by the textural structures, particularly by those in the non-crystalline regions both of the oriented and the unoriented specimens. However, further consideration of this problem is not given in this paper.

It is concluded that the orthorhombic crystal structure of PE is sustained under high pressures. This is firstly because of the fact that no sign of split of the diffraction lines, which should be expected by the transformation of the basal lattice plane from the orthogonal for PE to an oblique structure, was observed by the pressure applications. This conclusion was further checked by the following calculations.

For the orthorhombic structure the interplanar spacing d_{hkl} for a plane (hkl) can be calculated by the relation

$$\frac{1}{d_{hkl}^2} = \frac{h^2}{a^2} + \frac{k^2}{b^2} + \frac{l^2}{c^2} \qquad (6)$$

where a, b, and c are the unit cell parameters. If the orthorhombic structure remains, the following relation will be obtained for the small changes in the cell parameters,

$$\frac{1}{d_{hkl}^2} \cdot \varepsilon = \frac{h^2}{a^2} \varepsilon_a + \frac{k^2}{b^2} \cdot \varepsilon_b + \frac{l^2}{c^2} \cdot \varepsilon_c \qquad (7)$$

where ε, ε_a, ε_b, and ε_c are the fractions of the change of the spacing for the planes (hkl), ($h00$), ($0k0$) and ($00l$), respectively. For the 110 plane of PE, from eq 7, it follows

$$\varepsilon_{110} = 0.307\varepsilon_{200} + 0.693\varepsilon_{020} \qquad (8)$$

where Bunn's data[17] of a=7.40Å and b=4.93Å were used to obtain eq 8. The strains of the 110 plane were then calculated substituting ε_{200} and ε_{020} in the right-hand side of eq 8 by the experimental strains of eq 2 and 3 and compared with those observed. This is shown in Figure 8, where the calculated strain of the 110 plane appears to be slightly smaller than the observed. This small deviation is likely to be due to a systematic experimental error.

It is interesting to note that the orthorhombic crystal structure of PE is sustained under high pressures in spite of the anisotropic linear deformations in the a-axis and b-axis directions. This will be discussed in more detail later in the next section.

As was shown in Figure 10, the shifts of the 002 reflection by the pressure are so small that it is difficult to obtain a smooth curve for the pressure—strain relationship for the 002 plane. Since greater accuracy in measuring the $\Delta 2\theta$ was obtained for the 011 plane (Figure 12), whose normal is inclined 19 degrees to the c-axis, it will be safer to obtain the pressure—strain relationship for the c-axis direction from the following relations, using experimental results for the 011 and 020 planes.

$$\varepsilon_{c\text{-axis}} = 1.264\varepsilon_{011} - 0.264\varepsilon_{020} \qquad (9)$$

Substituting ε_{011} and ε_{020} in eq 9 by eq 5 and 3, $\varepsilon_{c\text{-axis}}$ was found to be represented by

c-axis (fiber axis) direction:

$$-\varepsilon_{c\text{-axis}} = 0.30 \times 10^{-6} p - 0.0032 \times 10^{-8} p^2 \qquad (10)$$

According to eq 10, at p=3000kg/cm^2, the value for $-\varepsilon_{002}$ of 0.00061 will be obtained which is

in agreement with the experimental value (0.0008).

DISCUSSION

Linear Compressibility

The anisotropy of deformation of the crystal lattice of PE along the three principal crystallographic axes under the hydrostatic compression can now be estimated quantitatively by comparing eq 2, 3, and 10 with each other. At $p=0$, the linear compressibilities, *i.e.*, the linear compressive strains per pressure of unity, represented by k's, are as follows at 20°C:

a-axis direction: $k_{200}=11.5\times10^{-6}\text{cm}^2/\text{kg}$

b-axis direction: $k_{020}=7.29\times10^{-6}\text{cm}^2/\text{kg}$

c-axis direction: $k_{c\text{-axis}}=0.30\times10^{-6}\text{cm}^2/\text{kg}$

The results for k_{200} and k_{020} can be shown to be in excellent agreement with the theoretical results by Odajima and Maeda,[20] who obtained $k_{a\text{-axis}}=13\times10^{-12}\text{cm}^2/\text{dyn}$ and $k_{b\text{-axis}}=7\times10^{-12}\text{cm}^2/\text{dyn}$. Consequently, the crystal lattice of PE is the most compressible in the a-axis direction and the most incompressible in the c-axis direction. It is 40 times more compressible in the a-axis direction than in the c-axis direction, 1.6 times more compressible in the a-axis direction than in the b-axis direction. Such anisotropic deformation of the crystal lattice of PE under hydrostatic compression was first described by Müller[1] for n-$C_{29}H_{48}$ and n-$C_{29}H_{60}$ crystals. He obtained the linear compressibilities due to a pressure of 1kg/cm^2 as, for n-$C_{23}H_{48}$, $k_{a\text{-axis}}=9.8\times10^{-6}$, $k_{b\text{-axis}}=10.8\times10^{-6}$, $k_{c\text{-axis}}<0.3\times10^{-6}$ and for n-$C_{29}H_{60}$, $k_{a\text{-axis}}=2.5\times10^{-6}$, $k_{b\text{-axis}}=3\times10^{-6}$, $k_{c\text{-axis}}<0.3\times10^{-6}$. Müller's results show basic agreement with the results on PE. Figure 14 and Table V are our results on the orthorhombic crystal lattice of n-$C_{27}H_{56}$. It is seen from Figures 13 and 14 that the 110 and the 200 planes of n-$C_{27}H_{56}$ behave, against pressures, in much the same way as the crystal lattice of PE. Müller carried out observations only at 1200 and 1400kg/cm^2 and his k-values along the a-axis and the b-axis directions of n-$C_{29}H_{60}$ may be pointed out to be too low.

The marked anisotropy manifested in the deformation of the crystal lattice of PE is due basically to its molecular constitution that, in the c-axis direction, it consists of fully extended carbon zigzags of covalent bonds, and in directions perpendicular to the c-axis (fiber axis), it consists of chain molecules packed by van der Waals forces. The mechanical anisotropy of the polymer crystals was thoroughly elucidated by the work of Sakurada and his coworkers[21,22] where an X-ray diffraction method was also applied to the oriented specimen under a uniaxial tensile direct load. Elastic moduli of the crystal lattice of polymers in the fiber axis direction (E_l) and those in the perpendicular direction to it (E_t), covering many kinds of crystalline polymers, were recently published.[21,22] According to the results of these authors, the anisotropy expressed by the ratio E_l/E_t ranges from 56 to 75 for PE, compared with that by hydrostatic comprssiion, $k_{200}/k_{c\text{-axis}}=40$, obtained in the present paper.

The observed ratio k_{200}/k_{020} of 1.6 is important,

Table VI. Mechanical anisotropy along the a-axis and the b-axis of polyethylene crystal[a]

	Author	Temp, °K	E_a	E_b	E_b/E_a	b_a	b_b	b_b/b_a
Theoretical	Ref 23	—	5.7	2.1	0.37	—	—	—
	Ref 5[b]	293	4.76	8.33	1.75	5.4	11.1	2.06
	Ref 5[c]	293	5.88	9.09	1.54	7.5	13.2	1.75
	Ref 24	0	9.44	8.56	0.91	—	—	—
Experimental	Ref 25	293	3.1	3.8	1.2	—	—	—
	Ref 26[d]	R[e]	2.5	1.9	0.76	—	—	—
	Present work	293	—	—	—	8.7	13.7	1.58

[a] Unit of dyn/cm$^2\times10^{10}$ was used. Subscripts a and b mean the a-axis and the b-axis directions, respectively. [b] Based on the potentials "Set I." [c] Based on the potentials "Set III." [d] Numerical data were taken from ref 5. [e] Room temperature.

because views on mechanical anisotropy of PE crystal along the *a*-axis and *b*-axis directions are varied, as illustrated in Table VI, where E stands for elastic modulus of uniaxial elongation and b linear bulk modulus of hydrostatic compression, *i.e.*, the reciprocal of linear compressibility. We only suggest that, experimentally, the result $b_{020}/b_{200}=1.6$ is justified on the basis of two X-ray films on which the 110, 200, 210, 020, 120, and 310 reflections were simultaneously observed and clearly recorded. One of them is shown in Figure 7 and the other for the 100°C-annealed drawn specimen in ref 14. A 50-hr experiment was necessary for each of them.

According to our previous experiments[27] using uniaxial compression, elastic moduli of 3.6×10^4 kg/cm^2 along the *a*-axis direction and 4.4×10^4 kg/cm^2 in the normal direction to (110) were obtained. The anisotropy between the two linear bulk moduli by hydrostatic compression of $b_{110}/b_{200}=1.32$ is qualitatively in agreement with the above results by uniaxial compression.

Further comparison of the linear compressibility seems difficult to make.

It should be mentioned that the anisotropy of the linear compressibilities of PE crystal lattice along the *a*-axis and the *b*-axis directions agrees with that of thermal expansions in the two directions shown by Swan,[28] $\alpha_{a\text{-axis}}=22\times10^{-5}$/°C and $\alpha_{b\text{-axis}}=3.8\times10^{-5}$/°C. The generally accepted reason for the latter case is the transformation from the orthogonal to the hexagonal packing of the molecular chains due to their thermal motions about their axes. Moreover, it is estimated[4] that the bulk compressibility of the crystal of polymers around room temperature consists of a 90-% contribution by the term of the lattice potential energy and only a 10-% contribution by that of the lattice thermal energy. Thus Kaji pointed out[29] that it is unreasonable to associate the anisotropy of thermal expansion of the PE crystal with its mechanical anisotropy of linear compressibility found in this paper.

Bulk Compressibility

The procedure to obtain volumetric compression of the crystal lattice *vs.* pressure relationship is simple for the orthorhombic structure of PE, because it can be deduced simply by summing up ε_{200}, ε_{020}, and $\varepsilon_{c\text{-axis}}$ obtained in eq 2, 3, and 10. It follows that

$$-\Delta V/V_0=19.1\times10^{-6}p-0.143\times10^{-8}p^2 \quad (11)$$

Eq 11 gives the pressure—volume relation of the crystal lattice of PE at 293°K, where V_0 is the volume under the normal pressure which is calculated, by using Swan's data,[28] to be 0.9994 cm^3/g. The isothermal compressibility, designated by β, is defined by eq 12.

$$\beta=-\frac{1}{V_0}\left(\frac{\partial V}{\partial p}\right)_T \quad (12)$$

By differentiating of eq 11 with respect to p, the compressibility—pressure relationship can be deduced as follows.

$$\beta\,[(\text{kg/cm}^2)^{-1}]=19.1\times10^{-6}-0.286\times10^{-8}p \quad (13)$$

According to eq 13 the compressibility of the crystal lattice of PE decreases linearly with increase in pressure. At $p=0$ it is 19.1×10^{-6} cm^2/kg, which is again in excellent agreement with the theory of Odajima and Maeda.[5] These authors obtained $\beta=1.99\times10^{-11}$cm^2/dyn ($=19.5\times10^{-6}$cm^2/kg) on the basis of the model of the Reuss' average (uniform stress model) and the potentials designated as "Set III." Indeed, the agreement between the theoretical predictions by Odajima, *et al.*, and our experimental results for linear as well as bulk compressibilities is very close and this indicates that the Reuss' average model usually predominates in the hydrostatic compression of the bulk specimen of PE within a strain of about 3%.

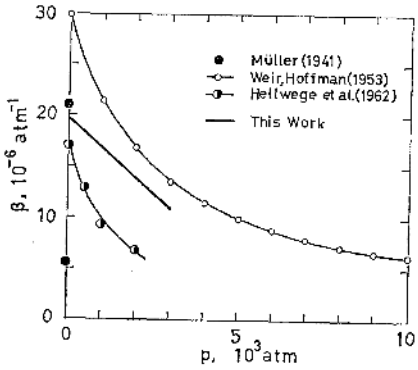

Figure 15. Pressure *vs.* compressibility relationship of the crystal lattice of PE compared with the results by Müller, by Hellwege, Knappe, and Lehmann and by Weir and Hoffman.

It is noted that the compressibility of the crystal lattice of PE has the same order of magnitude as the metallic sodium whose compressibility is reported[30] to be 16×10^{-6}cm^2/kg.

The result of compressibility expressed by eq 13 can further be compared with the experimental results obtained by Hellwege, Knappe, and Lehmann by means of piezometry.[8] This is shown in Figure 15. The above authors showed that the compressibility of PE of varying densities decreases linearly with increases in crystallinity. By extrapolation, using the data of these authors, the compressibilities of PE at 20°C corresponding to 100-% crystallinity, as expressed per pressure of 1kg/cm^2, can be shown to become approximately 16.5×10^{-6}, 12.5×10^{-6}, 9×10^{-6}, and 6.5×10^{-6} at pressures 1, 500, 1000, and 2000kg/cm^2, respectively. In Figure 15, the lattice compressibility of high-density PE under the normal pressure is seen to be larger by a factor of about 1.2 than the compressibility for the bulk specimen of 100-% crystallinity. The difference is not large and an essential agreement under normal pressure can be readily assumed. However, at $p=2000$kg/cm^2, the compressibility for the bulk specimen of 100-% crystallinity deviates greatly from the lattice compressibility, the former becoming half of the latter. Such a difference is clearly beyond experimental error and indicates a basic disagreement at high pressures.

In Figure 15 were also illustrated the results of compressibility for normal hydrocarbons obtained by Weir and Hoffman[7] by a piezometric method at 21°C. Weir, *et al.*, obtained these plots by averaging the compressibilities of the normal hydrocarbons of carbon numbers 18, 20, 24, 26, 28, and 30, which, according to the above authors, showed no difference in compressibility beyond experimental error. At normal pressure, the compressibility of the normal hydrocarbons, 29.8×10^{-6}atm^{-1}, is 1.56 times larger than the lattice compressibility of PE, while at $p=3000$atm, the difference becomes smaller, the former being 1.3 times larger than the latter. The initial higher compressibility on the side of the normal hydrocarbons may be attributed to the free space and/or voids which supposedly exist between crystal particles in the bulk of the specimen. At higher pressures, the space between chain ends *within* the crystal lattice of the hydrocarbons must now play a role for the residual difference, because, in directions perpendicular to the chain axis, it was shown that the crystal lattice of n-$C_{27}H_{56}$ shows almost the same lateral contraction against pressures as the high-density PE (Figure 14). For n-$C_{27}H_{56}$, measurements of the strains in the chain axis direction were unsuccessful in the present paper. Müller's result for n-$C_{23}H_{48}$ is found to be approximately the same as our results for PE, as seen in Figure 15.

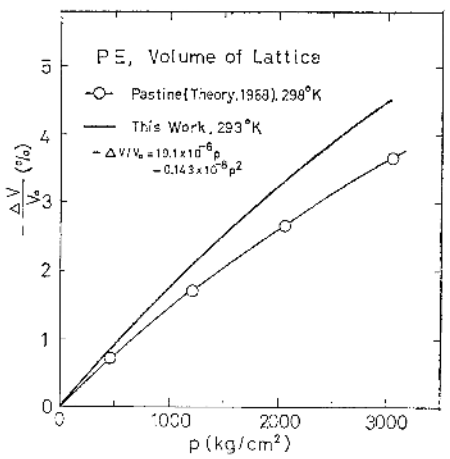

Figure 16. Pressure volume relation of the crystal lattice of PE compared with the theoretical results by Pastine.

It is worthwhile comparing eq 11 with the theoretical results calculated by Pastine[6] for purely crystalline PE at 298°K. Pastine's results, as shown by open circles in Figure 16, appear to be smaller than those observed, showing about 20-% deviation at $p=3000$kg/cm^2.

Anharmonicity

Another effective way to evaluate the pressure dependence of the $-\Delta V/V_0$ is to use the Grüneisen parameter and the C_2 parameter. Both parameters reflect the anharmonicity associated with the volumetric compression of solids.[31] The C_2 parameter is defined by Barker[8] as eq 14 for the first and second compressibility coefficients, a_1 and a_2, appearing in the expression in eq 15.

$$C_2=\frac{a_2}{a_1^2} \tag{14}$$

$$-\Delta V/V_0 = a_1 p + a_2 p^2 + a_3 p^3 + \cdots \quad (15)$$

Barker has shown, by analysing Weir's compression data[32] for several partially crystalline and noncrystalline polymers, that, for PE and most polymers, the C_2 parameter becomes -4.0 ± 0.1. For the crystal lattice of PE, the C_2 parameter is readily found by eq 11 to become -3.92, in surprising coincidence with Barker's conclusion on the bulk compression of polymeric solids. Such coincidence is of particular interest, because it means that the C_2 parameter, and therefore the Grüneisen parameter for the reason described later, is not sensitive to the textural structure of polymeric solids.

It should be noted that the C_2 parameter, if it can be applied to the linear compression, is larger by 2.5 times in the a-axis direction ($C_2 = -9.0$) than in the b-axis direction ($C_2 = -3.6$), as may be calculated from eq 2 and 3. This indicates that the anharmonicity associated with the linear compression of the PE crystal is larger in the a-axis direction than in the b-axis direction. It is also interesting to note that the linear compressibility in the a-axis direction, which is initially 1.6 times larger than that in the b-axis direction, decreases more rapidly than the latter with increases in pressure, and at a pressure over 2000kg/cm^2, the two cross. This will be shown from the first derivatives with respect to p of eq 2 and 3. These results observed on the linear compressibilities of the PE crystal should of course be related to the potential considerations and ought to be explained by the lattice dynamics such as are being promoted by Odajima and Maeda[5] and by Wobser and Blasenbrey.[24]

The Grüneisen parameter, γ, is defined in several ways.[33] For a purely crystalline PE, Pastine[6] slightly modified the Slater's original equation,[31] taking into account the predominant volume contraction in a plane perpendicular to the fiber axis, to give

$$\gamma = -\frac{1}{2} - \frac{1}{2} x \frac{\left(\dfrac{\partial^2 p_0}{\partial x^2}\right)}{\left(\dfrac{\partial p_0}{\partial x}\right)} \quad (16)$$

where $x = V/V_0$. Combining eq 16 with eq 15 and 14 and ignoring p^3- and higher p-terms in the former, it follows that

$$\gamma = -\frac{1}{2} - C_2 \quad (17)$$

Therefore, according to eq 17, which is obtained for a special case of $a_3 = a_4 = \cdots = 0$, the Grüneisen parameter is determined as the C_2 parameter is determined. It becomes, for the present work of the hydrostatic compression of the crystal lattice of PE, 3.4, a 30-% smaller value compared with the results (about 5 at 20°C) obtained by Wada and his coworkers[34] from the pressure dependence of the sound velocity using bulk specimens.

It should be pointed out that, in our investigations, it is desirable to extend the range of the pressures for observation, up to say, 10000 kg/cm^2. Experimental plots obtained at such very high pressures will add useful information about anharmonicity to those discussed above. Work along these lines is progressing in our laboratory.

Acknowledgment. The authors are grateful to Professor I. Sakurada of Doshisha University, and Professor F. Mashio and Professor H. Teranishi of this Faculty, for their continued interest and encouragement. They are indebted to Kobe Steel, Ltd., for help in the design and construction of the high-pressure cell and the pressure calibration of the high-pressure gauge, and wish to express their particular thanks to Professor T. Makita of Kobe University and Mr. T. Fukuda of Kobe Steel, Ltd., for their many valuable suggestions on high-pressure techniques.

This paper will be presented at the International Conference on the Mechanical Behavior of Materials, August 15—20, Kyoto, 1971, and part of it was presented before the Society of the Polymer Science, Japan,[14] and the Chemical Society of Japan.[15]

REFERENCES

1. A. Müller, *Proc. Roy. Soc.* (London), **A154**, 624 (1936); **A178**, 227 (1941).
2. W. Brandt, *J. Chem. Phys.*, **26**, 262 (1957).
3. R.E. Barker, Jr., *J. Appl. Phys.*, **38**, 4234 (1967).
4. M.G. Broadhurst and F.I. Mopsik, *J. Chem. Phys.*, **52**, 3634 (1970).
5. A. Odajima and T. Maeda, *J. Polym. Sci.*,

Part C, **15**, 55 (1966).
6. D.J. Pastine, *J. Chem. Phys.*, **49**, 3012 (1968).
7. C.E. Weir and J.D. Hoffman, *J. Res. Nat. Bur. Stand.*, **55**, 307 (1955).
8. K.-H. Hellwege, W. Knappe and P. Lehmann, *Kolloid-Z.Z. Polym.*, **183**, 110 (1962).
9. S.S. Kabalkina and L.F. Vereshchagin, *Dokl. Acad. Nauk SSSR*, **143**, 818 (1962).
10. T. Ito, Abstracts, SPSJ 18th Symposium on Macromolecules, Tokyo, November 13, 1969, p 571.
11. T. Ito and H. Marui, presented at the SPSJ 19th Symposium on Macromolecules, Kyoto, October 22, 1970.
12. K. Yasunami, *Nippon Kikai-gakkaishi* (*J. Japan Soc. Mech. Eng.*), **67**, 980 (1964).
13. K. Yasunami, *Metrologia*, **4**, 168 (1968).
14. T. Ito and H. Marui, Abstracts, SPSJ 19th Symposium on Macromolecules, Kyoto, October 22, 1970, p 889.
15. T. Ito and H. Marui, Abstracts, 12th Koatsu Toronkai (Symposium on High Pressure), Hiroshima, October 4, 1970, p 26.
16. H.P. Klug, *Ind. Eng. Chem. Anal. Ed.*, **12**, 753 (1940); H.P. Klug and L.E. Alexander, "X-Ray Diffraction Procedures," John Wiley, New York, N.Y., 1954, p 322.
17. C.W. Bunn, *Trans. Faraday Soc.*, **35**, 482 (1939).
18. J. Osugi and K. Hara, *Rev. Phys. Chem. Japan*, **36**, 28 (1966).
19. C.L. Gruner, B. Wunderlich and R.C. Bopp, *J. Polym. Sci., Part A-2*, **7**, 2099 (1969).
20. A. Odajima, private communication, 1970. Calculation was made on the basis of the results in ref 5. The potential designated there as "Set III" was used.
21. As a paper written collectively, see I. Sakurada, T. Ito, and K. Nakamae, *J. Polym. Sci., Part C*, **15**, 75 (1966).
22. I. Sakurada and K. Kaji, *J. Polym. Sci., Part C*, **31**, 57 (1970).
23. T. Miyazawa and T. Kitagawa, *J. Polym. Sci., Part B*, **2**, 395 (1964).
24. G. Wobser and S. Blasenbrey, *Kolloid-Z. Z. Polym.*, **241**, 985 (1970).
25. I. Sakurada, T. Ito and K. Nakamae, *Zairyo-shiken* (*J. Japan Soc. Testing Materials*), **11**, 683 (1962); T. Ito and I. Sakurada, Abstracts, SPSJ 11th Annual Meeting, Nagoya, May 26, 1962, p 19.
26. K. Kobayashi, Y. Taniguchi, I. Kimura, and S. Kimura, Abstracts, 15th Annual Meeting of the Chemical Society of Japan, Kyoto, April 2, 1962, p 129.
27. T. Ito, N. Sugiura and H. Kawai, *J. Polym. Sci., Part A-2*, **7**, 1439 (1969).
28. P.R. Swan, *J. Polym. Sci.*, **56**, 403 (1962).
29. K. Kaji, private communication, 1971.
30. A.V. Tobolsky, "Properties and Structure of Polymers," John Wiley, New York, N.Y., 1960, p 4.
31. J.C. Slater, "Introduction to Chemical Physics," McGraw-Hill, New York, N.Y., 1939, Chap. 13 and 14; C. Kittel, "Introduction to Solid State Physics," 3rd ed., John Wiley, New York, N.Y., 1966.
32. C.E. Weir, *J. Res. Nat. Bur. Stand.*, **46**, 207 (1951); **50**, 311 (1953); **53**, 245 (1954).
33. Y. Takagi in "Kesshō Butsurigaku (Physics of Crystal)," K. Ariyama, *et al.*, Ed., Kyoritsu Publishing Co., Ltd., Tokyo, 1957, pp 101—104.
34. Y. Wada, A. Itani, T. Nishi, and S. Nagai, *J. Polym. Sci., Part A-2*, **7**, 201 (1969).